

Ballistic quantum state transfer in spin chains: general theory for quasi-free models and arbitrary initial states

Leonardo Banchi^{1,2,3}

¹ Department of Physics and Astronomy, University College London, Gower St., London WC1E 6BT, United Kingdom

² Dipartimento di Fisica, Università di Firenze, Via G. Sansone 1, I-50019 Sesto Fiorentino (FI), Italy

³ INFN Sezione di Firenze, via G.Sansone 1, I-50019 Sesto Fiorentino (FI), Italy

November 8, 2018

Abstract. Ballistic quantum-information transfer through spin chains is based on the idea of making the spin dynamics ruled by collective excitations with linear dispersion relation. Unlike perfect state transfer schemes, a ballistic transmission requires only a minimal engineering of the interactions; in fact, for most practical purposes, the optimization of the couplings to the ends of the chain is sufficient to obtain an almost perfect transmission. In this work we review different ballistic quantum-state transfer protocols based on the dynamics of quasi-free spin chains, and further generalize them both at zero and finite temperature. In particular, besides presenting novel analytical results for XX, XY, and Ising spin models, it is shown how, via a complete control on the first and last two qubits of the chain, destructive thermal effects can be cancelled, leading to a high-quality state transmission irrespective of the temperature.

PACS. 03.67.Hk Quantum Communication – 75.45.+j Quantum tunneling in magnetic systems – 75.10.Jm Quantized spin models

1 Introduction

The development of novel experimental techniques capable of accessing and manipulating single quantum objects [1, 2, 3, 4, 5] has recently triggered a multifaceted interest towards the design of quantum devices and their components. Amongst them, a fundamental role is played by the channels used for connecting distant quantum information units, as they must supply high-quality quantum-state and entanglement transfer within the device.

When the quantum information is embodied in physical objects that one can move, the channel can simply be a path through which the carriers go undisturbed, as optical photons do through optical fibers. However this is not always the case, as many proposals for the realization of quantum devices are based on localized qubit, that need being connected by a further physical object, playing the role of a *wire*. In this paper we focus on this latter situation and, in particular, on the case of a wire made by a one-dimensional sequence of localized quantum systems, each statically interacting with its (nearest) neighbours. We further assume that the wire can be assembled with physical objects of the same type of those realizing the information units, so as to actually make reference to a network of qubits. In this setup, the transmission occurs thanks to the coherent collective dynamics of the components, rather than via a subsequent application of swapping gates. This feature was indeed one of the main motivation for introducing spin chains as many-body quantum wires [6, 7].

Quantum spin chains have a complex dynamics, featuring different phenomena, ranging from the spreading of the wave-function on different sites to the scattering between elementary excitations [8]. Consequently, if no control on these many-body phenomena is possible, a spin chain generally behaves as a very low-quality transmission channel for long distances [6, 9, 10]. In order to increase the transfer capabilities of a spin-chain data-bus different solutions have been proposed. Some are based on the idea of engineering the bus itself, by the specific design of its internal interactions [11, 12, 13]; others use the idea of intervening on the initialization process [10], by preparing the bus in a configuration found to serve the purpose; and still others use local or global dynamical control on the chain [14, 15]. In any case, a tough external action on the physical system is required. An alternative approach is that considering a data-bus made by a uniform spin chain which is weakly coupled to the external qubits [16, 17, 18]. In this setup, the transmission quality of quantum states and entanglement can be made arbitrarily high, provided the interaction between the bus and the qubits is arbitrarily small (see also [19, 20] for a related approach using strong magnetic fields). This proposal theoretically leads to near-to-perfect state transfer, meanwhile being experimentally feasible.

for some $N \times N$ dynamical matrices $U(t)$ and $V(t)$ which are obtained with a suitable transformation (see Appendix A) of the matrices A and B . Although the Jordan-Wigner mapping is non-local, the above equation (4) completely describe the dynamics of the boundaries of the spin chain. For instance, as $c_1(t) = \sigma_1^-(t)$ it is possible to obtain all the possible observables on the first site. Indeed, $\rho_1(t) = (1 + \mathbf{r}_1(t) \cdot \boldsymbol{\sigma}_1)/2$, with the *Bloch vector* elements

$$r_1^x(t) = \langle c_1^\dagger(t) + c_1(t) \rangle, \quad r_1^y(t) = -i\langle c_1^\dagger(t) - c_1(t) \rangle, \quad r_1^z(t) = 2\langle c_1^\dagger(t)c_1(t) \rangle - 1, \quad (5)$$

where the expectation values are taken over the initial ($t = 0$) state $|\Psi_{\text{in}}\rangle$. The state of the opposite spin $\rho_N(t) = (1 + \mathbf{r}_N(t) \cdot \boldsymbol{\sigma}_N)/2$, can be obtained in a similar way: the Wigner-string appearing in the mapping between $c_N(t)$ and $\sigma_N^-(t)$ can be written in terms of the parity $\Pi = \exp\left(i\pi \sum_{n=1}^N c_n^\dagger c_n\right) \equiv \prod_{n=1}^N (-\sigma_n^z)$ which is a constant of motion. Thereby one obtains $\sigma_N^-(t) = \Pi c_N(t)$ and

$$r_N^x(t) = \langle c_N^\dagger(t)\Pi + \Pi c_N(t) \rangle, \quad r_N^y(t) = -i\langle c_N^\dagger(t)\Pi - \Pi c_N(t) \rangle, \quad r_N^z(t) = 2\langle c_N^\dagger(t)c_N(t) \rangle - 1. \quad (6)$$

We focus on the quantum state transmission from the first qubit, sitting at site 1, to the one sitting at the opposite end of the chain, i.e. at site N . Hereafter these two qubits are referred to as the *sender* and *receiver*. Moreover, we call \bar{I} the chain composed by the spins localized in positions $2, \dots, N$. The internal chain acts as a noisy quantum channel which, in general, may alter, disperse or localize the state to be transferred. This noisy quantum channel can be described by a mapping $\rho_1(0) \rightarrow \rho_N(t)$. If the sender is not initially entangled with the rest of the system, namely if $|\Psi_{\text{in}}\rangle = |\Psi_1(0)\rangle \otimes |\Psi_{\bar{I}}(0)\rangle$, then the mapping takes the form of a simple linear relation between the initial and final Bloch vectors

$$\mathbf{r}_N(t) = D(t)\mathbf{r}_1(0) + \mathbf{d}(t). \quad (7)$$

The latter equation describes a qubit-to-qubit quantum channel [26], provided that $D(t)$ and $\mathbf{d}(t)$ satisfy some constraints [27,28]. In quasi-free quantum channels the 3×3 matrix $D(t)$ only depends on $U_{N1}(t)$ and $V_{N1}(t)$, while $\mathbf{d}(t)$ depends on $U(t)$, $V(t)$ and $|\Psi_{\bar{I}}(0)\rangle$ [10]. The matrix elements $U_{nm}(t)$ and $V_{nm}(t)$ describe the probability amplitude that a particle or a hole goes from site m to site n after a time t . Due to the relation between fermionic operators and spin ones at the boundaries, we show in the following that the transmission quality depends only on $u_1(t) = |U_{N1}(t)|$ and $v_1(t) = |V_{N1}(t)|$, provided that the initial state of the chain has a definite parity.

As a figure of merit for the transfer quality we use the optimal average transmission fidelity which is a measure of the fidelity between the initial state and the transmitted one. Before introducing this quantity, let us comment on a different strategy for quantum information transfer based on the teleportation protocol. Quantum teleportation allows the state transmission from the sender to the receiver not by directly injecting particles through quantum channels, but rather using local operations, classical communication, and an initially shared entangled state. In a spin chain setup, remote entanglement generation can be obtained by first creating entanglement locally, say between the spin 1 and a near auxiliary spin 0, and then sending ‘‘half of the state’’ (the state of spin 1) to the remote part (the spin N). If the ‘‘half-state’’ is perfectly transferred, then the result is a maximally entangled state between 0 and N at the transmission time, that is remote entanglement. However, the spin chain acts generally as a noisy quantum channel, and the resulting state is not maximally entangled. When the two remote parts share an entangled state, which is not maximally entangled, the fidelity of teleportation is not perfect [29,30]. One can show [30,9] that the average fidelity of state transmission is equivalent to the fidelity of the above protocol consisting of two steps: entanglement sharing and quantum teleportation. Owing to this equivalence, we only study quantum state transmission without considering the problem of entanglement transmission.

Quantifying the ability of a quantum channel to reliably transfer quantum information is a subject of active research [31]. Most figures of merit require the solution of complicated variational problems and are in general difficult to evaluate. Here we focus on a simpler quantity which does not measure the worst case scenario but rather the average transmission quality. An average state transmission fidelity can be defined as $\int d\psi_1 \langle \psi_1 | \rho_N(t) | \psi_1 \rangle$, and measures the fidelity between the initial state $|\psi_1\rangle$ of the sender and the (evolved) state of the receiver. If a perfect transfer is obtained for every initial state at a certain time t^* then $\int d\psi_1 \langle \psi_1 | \rho_N(t^*) | \psi_1 \rangle = 1$. However, in a spin chain setup, the external magnetic field may rotate the state $|\psi_1\rangle$ during the transmission. This effect is independent on the initial state and it is easily estimated and corrected via a local counter-rotation R . For this reason, in [10] the optimal transmission fidelity

$$F(t) = \max_{R \in \text{SU}(2)} \int d\psi_1 \langle \psi_1 | R^\dagger \rho_N(t) R | \psi_1 \rangle = \frac{1}{2} + \frac{\delta_1(t) + \delta_2(t) + \text{sign}[\det D(t)]\delta_3(t)}{6}, \quad (8)$$

has been introduced as a figure of merit for the transmission quality. In the above expression, $\delta_i(t)$ are the singular values of $D(t)$ sorted in decreasing order. The optimal counter-rotation R which maximizes the average fidelity cancels

the effects of the spin precession and it is independent on the particular initial state: it depends only on the model Hamiltonian, and as such can be estimated *a priori*.

For quasi-free one-dimensional spin models one obtains

$$F(t) = \frac{1}{2} + \frac{1}{6} |u_1^2(t) - v_1^2(t)| + \frac{p}{3} \max\{u_1(t), v_1(t)\}, \quad (9)$$

where $p = |\langle \exp(i\pi \sum_{n=2}^N c_n^\dagger c_n) \rangle| = |\langle \prod_{n=2}^N (-\sigma_n^z) \rangle|$ is the expectation value of the parity in the initial state $|\Psi_{\tilde{F}}\rangle$ of \tilde{F} . When $|\Psi_{\tilde{F}}\rangle$ has a definite parity, $p = 1$ and the transmission quality only depends on the dynamical amplitudes $u_1(t)$ and $v_1(t)$. Several initial states that are experimentally achievable [2,32,33] have a definite parity, notably the ground state, the fully polarized state, and the Néel state. On the other hand, when the chain \tilde{L} is in a thermal state with some inverse temperature β , then $p = \prod_k \tanh(\beta \tilde{E}_k/2)$ where \tilde{E}_k refers to the energy eigenvalues \tilde{L} . For this reason, the transmission quality can be significantly suppressed above a certain temperature threshold. In the worst case scenario, when $p = 0$, the fidelity is always lower than the classical value [30], i.e. $F < 2/3$, and there is no benefit in using a quantum data-bus. The non-local Wigner-string operator introduces entanglement between the boundary qubit N and the bulk which strongly suppresses the quality of transmission. In this regime the gap of the Hamiltonian sets the temperature threshold below which the initial state can be considered as the ground state, so with $p \simeq 1$. However, special attention is needed before trying to use a gapped Hamiltonian for increasing the maximum temperature. Indeed, known formulas for the Hamiltonian gap are usually obtained in the thermodynamic limit and for closed boundary conditions. It is important to stress that in open finite chains there could be some differences: for instance, the XY Hamiltonian is gapped for closed boundary conditions but there is an out-of-band mode in open chains which has exponentially small energy and makes the open XY Hamiltonian gapless [34]. However, taking into account features specifically arising from open boundary conditions, finite systems have generally a finite gap. Therefore, given a sufficiently low temperature, the initial state can be considered a pure state with definite parity. In sections 3 and 4 this approximation is assumed, while the constraints on the initial state are relaxed in Section 5.

3 Ballistic quantum information transfer with XX models

3.1 Perfect state transmission

In this section we study the state transmission in XX models, where $\gamma_n = 0$, the number of fermions in the initial states is conserved, and $V(t) = 0$. We show how to make an XX spin chain a perfect mirror via a suitable engineering of the coupling strengths j_n . Then we introduce a minimal engineering scheme where all the couplings are uniform $j_n = j = 1$ (j sets the energy scale) except at the boundaries, $j_1 = j_{N-1} \neq j$.

Hamiltonians acting as perfect dynamical mirrors have been introduced in [35,36]. With *ad-hoc* engineering of *all* the interactions, one can perfectly transfer not only the states between the ends of the chain, but also whatever state in position x to the position $N - x + 1$, N being the length of the chain. In order to understand what are the dynamical features of these chains let us consider an arbitrary initial state with $M < N$ spins in the state $|1\rangle$ and $N - M$ spins in the state $|0\rangle$. This state can be written as

$$|\psi\rangle = \sum_{\{m_1 < m_2 < \dots < m_M\}} \psi(\{m_n\}) \sigma_{m_1}^+ \sigma_{m_2}^+ \dots |0\rangle = \sum_{\{m_1 < \dots < m_M\}} \psi(\{m_n\}) c_{m_1}^\dagger c_{m_2}^\dagger \dots |0\rangle, \quad (10)$$

where $|0\rangle = |00\dots\rangle$ is the vacuum of the Fermi operators and where the ordering $m_1 < m_2 < \dots < m_M$ is required for removing the action of the Wigner string. After a certain time t ,

$$\begin{aligned} |\psi(t)\rangle &= \sum_{\{m_1 < \dots < m_M\}} \sum_{\{\ell_n\}} \psi(\{m_n\}) U_{m_1 \ell_1}^*(t) U_{m_2 \ell_2}^*(t) c_{\ell_1}^\dagger c_{\ell_2}^\dagger \dots |0\rangle \\ &= \sum_{\{m_1 < \dots < m_M\}} \psi(\{m_n\}) \sum_{\{\ell_1 < \dots < \ell_M\}} \det\{U_{m_j, \ell_k}^*(t)\} \sigma_{\ell_1}^+ \sigma_{\ell_2}^+ \dots |0\rangle, \end{aligned} \quad (11)$$

where $\det\{U_{m_j, \ell_k}^*(t)\} = \sum_{\pi} (-1)^\pi \prod_j U_{m_{\pi(j)}, \ell_j}^*(t)$ and the π 's refer to the permutation of the indices $\{\ell_n\}$. In the last equality we have chosen a proper order of the indices for mapping the many-fermion state back to the spin representation. A perfect transmission occurs if at a certain time t^* it is

$$U(t^*) = e^{i\alpha} X, \quad X_{nm} \equiv \delta_{n, N-m+1}, \quad (12)$$

where X is the reflection operator and α an arbitrary phase. If this is the case $|\psi(t^*)\rangle$ becomes

$$|\psi^{\text{mirrored}}\rangle = \sum_{\{m_1 < \dots < m_M\}} e^{i\alpha_{\{m_n\}}} \psi(\{N+1-m_n\}) \sigma_{m_1}^+ \sigma_{m_2}^+ \dots |0\rangle, \quad (13)$$

with a phase $\alpha_{\{m_n\}} = \frac{\pi}{2}\bar{n}(\bar{n}-1) - \bar{n}\alpha$, where \bar{n} is the number of fermions in the state. The phase $\alpha_{\{m_n\}}$ can be made constant in every sector with a definite parity by choosing, e.g., $\alpha = \pi/2$. In the XX model this can be done for instance with a proper choice of the magnetic field. Nevertheless, when $|\psi\rangle$ is a superposition of states with different parities, non-trivial effects can occur and the dynamics can generate an entangling gate [37,38].

An XX spin chain generates a dynamical mirror operator if Eq. (12) is satisfied. We now analyse what are the Hamiltonians whose dynamics satisfy Eq. (12) for some t^* . In the XX model, as $B = 0$ in Eq. (1), $U(t) = e^{-itA}$; so the first requirement for perfect transmission is that the hopping matrix A and the reflection matrix X have to be diagonal in the same basis, i.e.

$$[A, X] = 0. \quad (14)$$

The above condition requires a mirror-symmetric Hamiltonian. Indeed, the hopping matrix A has to be symmetric with respect to the ‘‘anti-diagonal’’, a property called *persymmetry* in the mathematical literature [39]: $j_n = j_{N-n}$ and $h_n = h_{N-n+1}$. Furthermore, calling ω_k the eigenvalues of A , Eq. (12) forces the existence of a time t^* such that $e^{-i\omega_k t^*}$ is proportional to the eigenvalues of X . If the energy eigenvalues ω_k are sorted in increasing order, then one can show [37] that Eq. (12) requires the following condition

$$e^{-i\omega_k t^*} = e^{i\alpha}(-1)^k, \quad (15)$$

where $(-1)^k$ are the eigenvalues of X . When the matrix A is persymmetric and the condition (15) holds, then perfect transmission is obtained between sites which are at the same distance from the opposite boundaries: the XX chain acts as a perfect dynamical mirror. Condition (15) can be solved numerically using inverse eigenvalue techniques, i.e. algorithms giving an Hamiltonian with the required spectrum [40,41]. Moreover, several analytic solutions of (15) have been found [12]. The simplest amongst these [42] requires no magnetic fields, $h_n = 0$, and a full engineering of the couplings according to the law $j_n \propto \sqrt{n(N-n)}$.

To the best of the author’s knowledge, all perfect state transfer schemes are based on fully engineered chains. These approaches are thus overwhelmingly complicated in an experimental perspective, as an experimentalist should be able to perform a fine tuning of the interactions according to, e.g., the law $j_n \propto \sqrt{n(N-n)}$. Moreover, the dependence on N of the coupling strengths avoids scalability: when the transmission distances are varied, all the nearest-neighbour interactions have to be changed as well.

In the next sections different models are introduced where the condition (15), though not exactly satisfied for each k , is accurately fulfilled by those modes which are relevant for the dynamics. Although condition (15) sets the fundamental requirement for achieving perfect state transmission with fully engineered models, it is also one of the main building blocks for ballistic quantum state transmission with minimally engineered models.

3.2 Minimal-engineered models and wave-like dynamics

Transferring quantum states from sender to receiver does not require the full mirror inversion of the whole chain. What is really needed is the swap of the boundary states irrespective of what happens to the rest of the chain. Therefore, condition (12) is overblown. The only requirement is that $u_1(t^*) = |U_{1N}(t^*)| \simeq 1$ for some transfer time t^* which should be as short as possible, i.e. $t^* = \mathcal{O}(N/\max_j |j_n|)$. How can this goal be accomplished and the unnecessary hypotheses relaxed? First of all it is known that the mirror-symmetry of the Hamiltonian, i.e. Eq.(14), is still a necessary prerequisite for the transmission between site 1 to N [12]. We thus consider mirror-symmetric Hamiltonians and write the spectral decomposition of the hopping matrix A as $A = O\omega O^T$. Then one can show [22] that

$$u_1(t) = \left| \sum_k O_{1k}^2 (-1)^k e^{-i\omega_k t} \right|, \quad (16)$$

where the identity $O_{1k} = \pm(-1)^k O_{Nk}$, which is a property of persymmetric matrices [39], has been used. The above equation shows that a high quality transmission can be obtained when the condition (15) is *approximately* satisfied by the modes k which mainly influence the dynamics, namely those for which O_{1k}^2 is significantly different from zero. This requirement can be fulfilled with a minimal engineering of the interactions. Minimally engineered models are a deviation from the uniform case and the resulting hopping matrix A is quasi-uniform [43]; therefore, the model can be diagonalized and its features expressed by means of shifted quasi-momenta $q \approx \pi k/N + \eta_k$, where $k = 1, \dots, N$ and the

shifts $\eta_k = \mathcal{O}(N^{-1})$ depend on the parameters of the non-uniform part of the Hamiltonian. Using the quasi-momentum q as an alternative index for k , one realizes that

$$u_1(t) \approx \left| \sum_q \varrho(q) e^{i[Nq - \omega_q t]} \right|. \quad (17)$$

where $\varrho(q) = \mathcal{O}_{1q}^2$. The above equation models a wave packet in momentum space which evolves with an energy ω_q that, being the model quasi-uniform, can be interpreted as a dispersion relation. Although ω_q can be a complicated function, a ballistic coherent quantum information transmission is obtained by designing the wave-packet in momentum space in such a way that $\varrho(q)$ is peaked around the inflection point of the dispersion relation, i.e. where $\omega \approx vq$ for some group velocity v . Indeed, in this case $u_1(t \simeq N/v) \approx \sum_q \varrho(q) = 1$.

A “wave-packet encoding” scheme suitable for quantum communication has been proposed also in [44, 45]. However, in that case the wave-packet is created in real space by encoding the state to be transferred into a wave-packet over multiple sites of the chain. Classical wave dynamics theory is then exploited for designing the optimal shape of the packet so as to minimize the dispersion. On the other hand, the minimal-engineering approach does not require the control of multiple sites for the encoding, as the wave-packet is not formed in the site-space but rather in the quasi-momentum space. Indeed, the non-uniform interactions make the system not diagonalizable by a Fourier transform, and the resulting wave-packet shape $\varrho(q)$ can be tuned, as shown below, by acting on the non-uniform part of the Hamiltonian.

In [21, 22] the simplest Hamiltonian suitable for high-quality ballistic quantum state transmission has been found. The model consists of an XX spin chain with no applied magnetic field, $h_n = 0$, and

$$j_n = 1, \text{ for } n = 2, \dots, N-2, \quad j_1 = j_{N-1} \neq 1. \quad (18)$$

This particular choice of minimal couplings is natural for applications. Consider for instance a potential implementation in a quantum device: sites 1 and N are part of two distant quantum registers, while the rest of the chain models the physical medium for connecting them. When the sender’s state has to be transferred to the receiver, the interaction j_1 is switched on and the (many-body) dynamics of the chain is then used for mediating the transmission. As in a potential application the couplings $j_1 = j_{N-1}$ must be controllable, it is natural to require that they could also be switched on and set to a specifically tuned value which is different from the other couplings of the chain. The XX model with non-uniform interactions (18) can be solved analytically: the dispersion relation reads

$$\omega_q = \cos q, \quad (19)$$

where the quasi-momentum q takes N discrete values q_k in the interval $(0, \pi)$:

$$q_k = \frac{\pi k + 2\varphi_{q_k}}{N+1}, \quad \varphi_q = q - \cot^{-1}\left(\frac{\cot q}{\Delta}\right) \in \left(-\frac{\pi}{2}, \frac{\pi}{2}\right), \quad \Delta = \frac{j_1^2}{2 - j_1^2}. \quad (20)$$

The corresponding shape of the wave-packet $\varrho(q)$, namely the density of the excitations, is

$$\varrho(q) = \frac{1}{N+1-2\varphi'_q} \frac{\Delta(1+\Delta)}{\Delta^2 + \cot^2 q}. \quad (21)$$

Eqs.(19) and (21) show a peculiar property of this quasi-uniform XX chain: the dispersion relation is almost linear around the zero-energy zone and the density of the excitations $\varrho(q)$ is peaked around this zone. The width of this peak is described by Δ and decreases for decreasing j_1 .

In the limit of very weak j_1 only the zero-energy modes are involved in the dynamics [17, 46, 16, 18]. In this regime the dynamics is basically a resonant transmission mediated by one mode. Indeed, when $j_1 \ll 1$ one can use perturbation theory for tracing out the off-resonant modes and obtain an effective Hamiltonian acting on the boundaries [17]. The strength of the resulting long-distance effective interaction is very weak (much weaker than j_1) and consequently the resulting transmission times are very long and non ballistic.

On the other hand, a coherent ballistic transmission must be a non-perturbative phenomenon. When j_1 increases, more and more normal modes are involved and resulting dynamics emulates a wave packet, as in Eq.(17). The fundamental observation is that a narrow $\varrho(q)$ is not the only requisite. Indeed, as the model is not translationally invariant, the phase-shifts in the quasi-momenta can alter the dispersion relation for very weak j_1 . The explicit calculation of the group velocity of the wave-packet around the linear zone reads [22]

$$v \propto \partial_k \omega_{q_k} = \frac{\pi}{t^*} \left[1 + \left(2 \frac{1-\Delta^2}{t^* \Delta^3} - \frac{1}{2} \right) \cos^2 q_k + (\cos^4 q_k) \right], \quad (22)$$

where $t^* = N+1 + 2(1-\Delta)/\Delta$ is the arrival time. Being the wave-packet peaked around the linear zone, the first non-linearity comes from the cubic terms of ω_q and depends on both N and j_1 . The dispersive term can be minimized via an optimal choice of $j_1 = \mathcal{O}(N^{-1/6})$. This is the reason for the existence of a *non-weak* optimal value [21] ensuring a coherent ballistic transmission.

From a quantitative point of view it is found that the optimal values j_1^{opt} are not those minimizing the dispersive term in (22). Indeed those optimal values come from a trade-off of two competing requirements

1. $j_1^{\text{opt}} < j_1^{\text{w}}$, where j_1^{w} represent the optimal coupling for making the width of the wave packet significantly different from zero only around the linear zone.
2. $j_1^{\text{opt}} > j_1^{\ell}$ where j_1^{ℓ} represents the threshold below which the “linear zone” is no more linear, as shown in Eq. (22).

These two competing effects cannot be efficiently managed via a single parameter j_1 : the optimal coupling is a compromise, and is found to scale as $j_1^{\text{opt}} = \mathcal{O}(N^{-1/6})$. When the optimal coupling is used the obtained transmission fidelity is above 95% for $N \approx 100$ and $F > 90\%$ even in the thermodynamic limit [21,22]. The advantages of the coherent ballistic dynamics are evident: only the couplings j_1 need to be controlled, there is no need for engineering, nor for controlling many qubits for encoding a wave-packet and, thanks to the non-weak couplings, transmission times are fast.

The two competing constraints discussed above are a general feature of minimally-engineered models and in [24] it has been shown that they can be overcome by introducing another optimally tuned value $j_2 = j_{N-2}$. We will discuss this point in detail in Section 5, while in the next section we study how to induce a ballistic quantum information transfer in particle non-conserving models.

4 Minimal engineering of the XY model

We have shown that the problem of transferring a quantum state in an XX spin chain is equivalent to the transmission of a fermion in one dimension and we have optimized such transmission using minimal requirements. The main guideline of the optimization procedure is to tune the interactions such that the travelling fermion generates a wave-packet whose shape in the quasi-momentum space can be controlled by the boundary couplings. By tuning that shape around the linear zone of the dispersion relation a coherent ballistic dynamics occurs. In this section we extend this approach to the XY spin model, whose Hamiltonian can be mapped into the fermionic Hamiltonian (1). Unlike the XX case, the total magnetization along the z direction is not a constant of motion and, as $B \neq 0$, the dynamics does not conserve the number of fermions in the initial state. Nonetheless the model can still be diagonalized by a canonical Bogoliubov transformation, and written into a set of independent (non-interacting) fermionic modes. With some technical modifications the minimal optimization procedure can be applied even in this case.

As in the previous section, before introducing the simplest engineering, we state some general comments about the properties that an XY Hamiltonian should satisfy in order to act as a (quasi) perfect quantum state transmitter. For the sake of simplicity, we consider $\gamma_n = \gamma j_n$. An XY spin chain acts as a perfect mirror if $U(t^*) = e^{i\alpha} X$, for some α and $V(t^*) = 0$ at the transmission time t^* ; models where this condition occurs have been studied in the literature [13,47], and are known to require the full engineering of the couplings j_n , plus a further control on the local magnetic field h_n .

Proceeding as in the XX case we here study how the conditions required for a perfect mirroring of the whole chain can be reduced if one rather aims at obtaining a high quality state transmission. In Appendix A, and in particular in Appendix A.1, we analyse the role of the symmetries. It is shown that the mirror-symmetry is a fundamental condition both for operating as a perfect dynamical mirror and for transferring states between sender and receiver. Therefore, we assume the mirror-symmetry also for the XY spin chain. Due to this symmetry, as shown in Appendix A.2, it is

$$U_{1N}(t) = \sum_k \left[\left(\frac{W_{k1} + s_k W_{kN}}{2} \right)^2 s_k e^{-i\omega_k t} - \left(\frac{W_{k1} - s_k W_{kN}}{2} \right)^2 s_k e^{i\omega_k t} \right], \quad (23a)$$

$$V_{1N}(t) = \sum_k \left(\frac{W_{kN}^2 - W_{k1}^2}{4} \right) s_k (e^{-i\omega_k t} - e^{i\omega_k t}), \quad (23b)$$

where W is an orthogonal matrix required to define the canonical transformation that diagonalizes the Hamiltonian, ω_k are the corresponding energies, and $s_k = (-1)^k$. It turns out that $W_{k1} \simeq \pm(-1)^k W_{kN}$. These relations are exact in the XX case and are true, though with some approximation, also in the XY case in the most relevant cases, namely when it is found $U_{N1}(t^*) \approx 1$ and $V_{N1}(t^*) \approx 0$ at the transmission time t^* . Consequently, the approximated evolution operator $u_1(t) = |U_{N1}(t)|$ is

$$u_1(t) \approx \left| \sum_k \varrho(k) e^{i(\pi k - \omega_k t)} \right|, \quad \varrho(k) = W_{k1}^2. \quad (24)$$

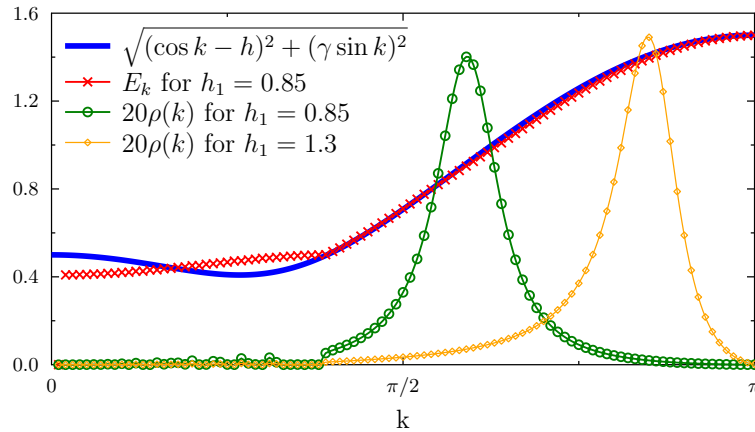


Fig. 1. Dispersion relation, energies ω_k and density of excitations for $N = 100$, $\gamma = h = 0.5$ and $j_1 = j_{N-1} = 0.48$. The peak of the density $\varrho(k)$ can be controlled by the local magnetic field: it turns out that the energy value of the peak is basically given by $h_1 = h_N$, i.e. by the local energy. The seemingly bad agreement between ω_k and the dispersion relation, in the left side, is due to the numerical increasing ordering of the eigen-energies ω_k .

The above equation proves that, due to the mirror symmetry, the dynamics can be described as a wave-like evolution travelling from sender to receiver also in the XY case. Although approximated, Eq. (24) has the same form of Eq. (16), which is valid for the XX case. The difference stems from the shape of the wave-packet in the momentum space $\varrho(k) = W_{1k}^2$ which is slightly more complicated because of the different diagonalization procedure (see Appendix A.2). In the following we investigate how one can obtain an almost perfect transmission in XY chains. Some numerical findings about XY spin chains that operate as coherent ballistic channels have already been obtained in [23, 21].

The achievement of a coherent dynamics in the XY model begins, as in the XX case, with the analysis of the dispersion relation in the infinite chain limit,

$$\omega_k = \sqrt{(h - \cos k)^2 + \gamma^2 \sin^2 k}, \quad (25)$$

displayed in Fig. 1. One can easily spot the existence of a region of linearity in the neighborhood of the inflection point(s) k_0 , where $\omega_k \approx \omega_{k_0} + v(k - k_0)$. It turns out that a local magnetic field $h_1 \simeq \omega_{k_0}$ allows the peak of $\varrho(k)$ to be centered around k_0 (see e.g. Fig. 1). The physical reason behind the possibility of changing the peak position via h_1 is more clear in the weak coupling limit. Indeed, when $j_1 \ll 1$ only the modes which are almost resonant with the local energy h_1 of the external qubits are involved in the dynamics. On the other hand, when j_1 increases more modes come into play and the peak is found to widen without changing its position. An optimal width can be determined numerically by finding the optimal coupling j_1^{opt} . An optimal coupling is indeed expected to emerge, as in the XX case, from a compromise between making $\varrho(k)$ peaked around k_0 and minimising the non-linearities introduced in ω_k around k_0 by the non-uniform interactions.

There are two main differences between XX and XY models. The first one is that, in the latter case, the region of linear dispersion depends on the parameters (γ and h): it sensibly shrinks as the anisotropy γ increases (which might make the bus useless) and can be extended by increasing the field h . For example, in the “extreme” case of the Ising chain ($\gamma = 1$), when $h = 0$ the dispersion relation becomes flat and does not allow for propagation. This explains the observation [9] that in such limit no entanglement propagation takes place: indeed, a vanishing group velocity means that nothing can be transmitted over the chain. However, a wide linear region can yet be obtained by applying a finite magnetic field h and one can act on the latter parameter so as to fulfil the conditions for optimal dynamics. The second important difference is the need for an extra parameter, i.e. the local magnetic field. In the XX case (say for $h = 0$) we have seen that the inflection point $k_0 = \pi/2$ corresponds to $\omega_{k_0} = 0$. There is no need for an extra local magnetic field because $\varrho(k)$ is already peaked around the mode with zero energy, which is notably also the center of the linear zone. On the other hand, the dispersion relation of the XY model (25) is gapped and $\omega_{k_0} \neq 0$. Unlike the XX case, when the XY model is considered, one has to switch on a local magnetic field $h_1 \simeq \omega_{k_0}$ in order to increase the average energy of the initial state and make $\varrho(k)$ peaked around the linear zone. In XY models the analytical expressions are more complicated as the Hamiltonian cannot be expressed in terms of symmetric quasi-uniform tridiagonal matrices [43], so the optimal parameters have to be found numerically [23, 21]. In the following we analyse the transmission in an Ising model ($\gamma = 1$) where, on the other hand, some analytical calculations can be performed.

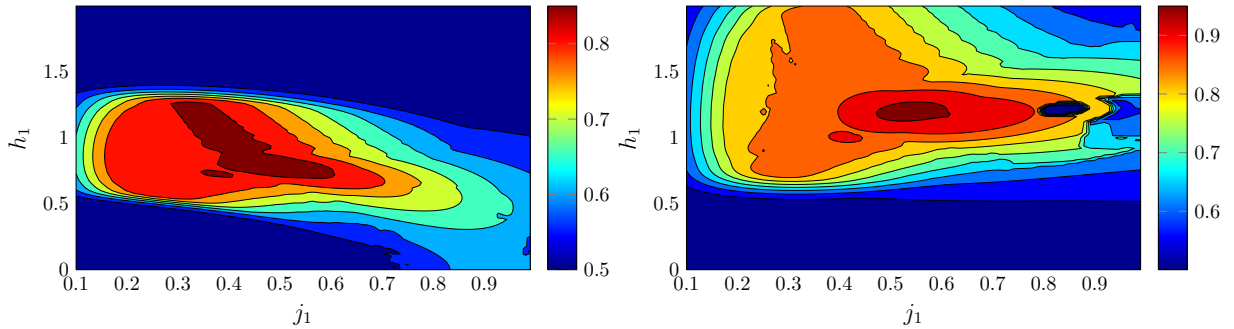


Fig. 2. Contour plot of the fidelity of transmission $F(t^*)$ for $N = 50$, $\gamma = 1$, $h = 0.5$ (left) and $h = 1.5$ (right). The transmission times have been obtained by maximizing the $F(t)$ for ballistic times, i.e. when $t \approx N/v$, being $v = \min\{h, h^{-1}\}$ the group velocity around the linear zone. The plots show the optimal value of j_1 and h_1 and the corresponding high fidelity.

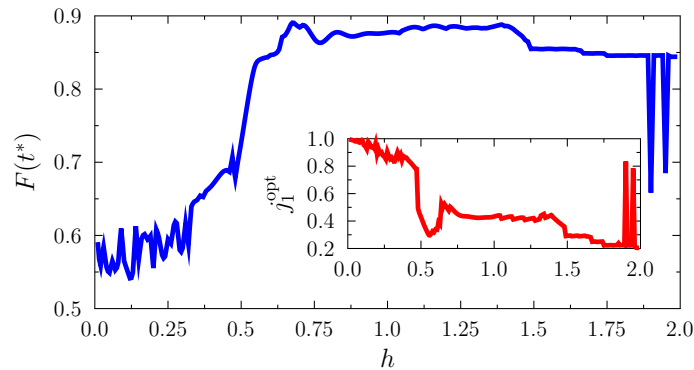


Fig. 3. Transmission fidelity for different h , $N = 50$, $\gamma = 1$ and $h_1 = h$. The inset shows the corresponding optimal values j_1^{opt} .

4.1 Ising case

The Ising chain with non-uniform interactions can be analytically diagonalized: the matrix $Z Z^T$, being $Z = A - B$ (see Eq. (1) and appendix A), is a quasi-uniform tridiagonal matrix with non-uniform corners. Thanks to the results of [43] one can show that for $N \gg 1$ the eigenvalues of $Z^T Z$ are $\omega_k^2 = 1 + h^2 - 2h \cos k$, i.e. the square of the dispersion relation (25). Taking the quasi-momentum operator k as an alternative index one can show that

$$\varrho(k) \propto \frac{j_1^2 \sin^2 k}{[(2-j_1^2) \cos k - x]^2 + j_1^4 \sin^2 k}, \quad x = \frac{1 + h^2 - h_1^2 - j_1^2}{h}. \quad (26)$$

The peak of $\varrho(k)$ is obtained for $k_0 = \cos^{-1} \frac{x}{2-j_1^2}$, while the energy of the mode k_0 is

$$\omega_{k_0} = \sqrt{1 + h^2 - 2h \cos k_0} = \sqrt{\frac{2h_1^2 + (1-h^2)j_1^2}{2-j_1^2}}, \quad (27)$$

and the width of the peak is given by

$$\Delta = \frac{j_1^2}{\sqrt{(2-j_1^2)^2 - x^2}}. \quad (28)$$

In the limit $j_1 \rightarrow 0$ the resonant mode is the one with energy $|h_1|$, as expected; however, for finite j_1 , a shift is observed. Moreover, it turns out that $|W_{kN}| = \frac{h_1}{\omega_k} |W_{k1}|$; when $h_1 \simeq \omega_{k_0}$, as we are interested in the neighbourhood of the resonant mode, we can neglect the prefactor and consider $|W_{k1}| \simeq |W_{kN}|$: this is an analytical proof of the validity of the approximated formula (24).

For making the optimal dynamics to emerge, the position of the peak must be centered around the linear zone of the dispersion relation $\bar{\omega} = \sqrt{|1-h^2|}$, i.e. $\omega_{k_0} = \bar{\omega}$. This condition is satisfied by setting

$$h_1 = \begin{cases} \sqrt{(1-j_1^2)(1-h^2)} & \text{for } |h| \leq 1, \\ \sqrt{h^2-1} & \text{for } |h| \geq 1, \end{cases} \quad (29)$$

and the corresponding width is

$$\Delta = \frac{\max\{|h|, 1\}}{\sqrt{|1-h^2|}} \frac{j_1^2}{2-j_1^2}. \quad (30)$$

The above reasoning cannot be applied at the “critical” value $h = 1$, as it predicts $h_1 = 0$. However, $h_1 = 0$ corresponds to $W_{kN} = 0$, $u_1(t) = v_1(t)$ and yields a very low transmission fidelity. Notice that the width Δ has a prefactor, as compared with the XX case, which is greater than 1. The optimal j_1 is then expected to be smaller than the XX counterpart.

In Fig. 2 we plot $F(t^*)$ for different parameters and show that the fidelity for the optimal values of j_1 and h_1 exceeds 95% for a chain of 50 spins when $h = 1.5$ while it is slightly lower for $h = 0.5$. In both cases the optimal values are quite in agreement with the estimate (29), although the latter has been obtained after different approximations.

The above analysis has been obtained by looking only at the density of the excitations, without considering the perturbations of the dispersion relation due to the local non-homogeneous coupling j_1 and magnetic field h_1 . However, these non-homogeneous terms introduce a shift in the quasi-momenta [43] that alters the dispersion relation. In the XX case, we have seen that this effect can transform the linear zone into a dispersive one. In principle, even the opposite could happen: the quasi-momenta shift due to the non-homogeneous interactions might linearize ω_k around a certain k_0 , ultimately making the dynamics more coherent. We have numerically observed that the phase shift mostly affects ω_k around the peak k_0 of $\rho(k)$. Therefore, we have performed a numerical simulation without considering the optimization of h_1 : even if the resulting $\rho(k)$ is not peaked around the linear zone, the subsequent optimization of j_1 can slightly linearize ω_k around k_0 . The results of the numerical analysis with $h_1 = h$ are shown in Fig. (3). As expected, the transmission fidelity is lower compared to the case where even the position of k_0 is optimized via h_1 . Nonetheless, for $h > 0.6$ the transfer quality is considerably high.

5 Minimal encoding for reliable transmission regardless of temperature and initial state

The minimal engineering scheme introduced in the previous section has the advantage of requiring only the ability to address the boundary qubits and to switch on the couplings between the boundaries and the bulk to an optimal non-perturbative value. With these minimal requirements an XY spin chain acts as a reliable transmission channel with fast transmission times $t^* = \mathcal{O}(N/j)$. Depending on the physical implementation, the optimal dynamics can be improved if one can address and manipulate the couplings between two further qubits, i.e. if one can operate locally on the qubits $1, 2, N-1, N$. In [24] indeed it has been shown that the two constraints for obtaining the optimal dynamics discussed in Section 3.2 can be better satisfied by tuning a second parameter $j_2 = j_{N-2}$. Provided that the initial state of the chain \tilde{T} has a definite parity, by properly tuning $j_1 = \mathcal{O}(N^{-1/3})$ and $j_2 = \mathcal{O}(N^{-1/6})$ one obtains a fidelity higher than 99% for $N \rightarrow \infty$. This two-coupling engineering is not just a step towards the full engineering of the chain: the need for a further parameter arises from the requirement that two constraints have to be satisfied.

The ability to address four qubits (two on the left and two on the right) also permits one to disentangle the transmission from the initial state of the internal chain [48] and then make the transmission independent of $|\Psi_{\tilde{T}}(0)\rangle$. Although XY models are quasi-free, the spin operator $\sigma_N^- = II c_N$ is non-local in the fermionic picture because of the parity operator II . The latter makes the transmission strongly dependent on the initial state of the bulk [22]: if $|\Psi_{\tilde{T}}(0)\rangle$ does not have a definite parity, then there is a destructive interference which strongly suppresses the transmission. With a suitable four-qubit protocol, such a destructive interference is cancelled. Similar schemes have also been proposed for achieving quantum state transfer in systems at high (infinite) temperature [18, 49, 50, 51].

We briefly discuss here the protocol introduced in [48], while in the following section we extend this algorithm to make it suitable for ballistic state transfer schemes. Consider the initial state $\rho_1(0) = (1 + \mathbf{r}_1 \cdot \boldsymbol{\sigma})/2$, parametrized by the Bloch vector \mathbf{r}_1 . This state can be encoded onto the state $\rho_{12}(0)$ of qubits 1 and 2 in two different ways (\pm)

$$\rho_{12}^{\pm}(0) = \frac{I_{\pm,12} + r_1^x \sigma_{\pm,12}^x + r_1^y \sigma_{\pm,12}^y + r_1^z \sigma_{\pm,12}^z}{2}, \quad (31)$$

$$\rho_{12}^-(0) = \frac{1}{2} \begin{pmatrix} 0 & 0 & 0 & 0 \\ 0 & 1+r_1^z & r_1^x - ir_1^y & 0 \\ 0 & r_1^x + ir_1^y & 1-r_1^z & 0 \\ 0 & 0 & 0 & 0 \end{pmatrix}, \quad \rho_{12}^+(0) = \frac{1}{2} \begin{pmatrix} 1+r_1^z & 0 & 0 & r_1^x - ir_1^y \\ 0 & 0 & 0 & 0 \\ 0 & 0 & 0 & 0 \\ r_1^x + ir_1^y & 0 & 0 & 1-r_1^z \end{pmatrix}, \quad (32)$$

where the above matrices are written in the computational basis $|\alpha\beta\rangle$, $\alpha, \beta \in \{0, 1\}$, and where \pm concerns the parity of the two-qubit state: ρ_{12}^+ (respectively ρ_{12}^-) refers to the state encoded into the subspace where $\sigma_1^z \sigma_2^z$ is positive

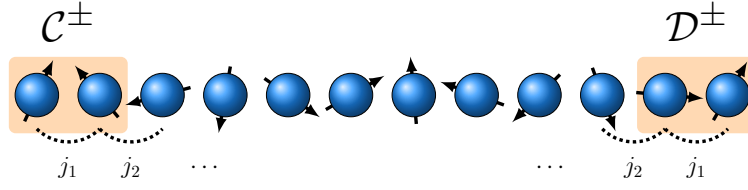


Fig. 4. Schematic representation of the state transfer protocol with the two-qubit encoding. With the proper coding operation \mathcal{C}^\pm and decoding operation \mathcal{D}^\pm one can make the result of the transmission independent of the initial state of the spins $2, \dots, N-1$. The couplings $j_n = j$ are uniform except that at the boundaries where they take the value j_1 and j_2 .

(negative). The operators encoding the qubits according to the above formulae read

$$I_{\pm,12} = \frac{1 \pm \sigma_1^z \sigma_2^z}{2}, \quad \sigma_{\pm,12}^x = \frac{\sigma_1^x \sigma_2^x \mp \sigma_1^y \sigma_2^y}{2}, \quad (33)$$

$$\sigma_{\pm,12}^y = \frac{\sigma_1^y \sigma_2^x \pm \sigma_1^x \sigma_2^y}{2}, \quad \sigma_{\pm,12}^z = \frac{\sigma_1^z \pm \sigma_2^z}{2}. \quad (34)$$

When perfect state-transfer Hamiltonians are used [48] the state ρ_{12}^\pm is perfectly transferred to the opposite end; at the transmission time t^* one obtains $\rho_{N,N-1}(t^*) = \rho_{12}^\pm$. The encoded state (31) is local in the fermionic picture and the transmitted state depends only on the operators $c_N(t^*)$ and $c_{N-1}(t^*)$, as well as on their Hermitian conjugate; having mapped the evolution into the transmission of two fermions the parity is automatically removed. Nevertheless, when the quality of transmission is not perfect, the transmitted state $\rho_{N,N-1}(t^*)$ may not have a definite two-qubit parity, making the decoding procedure more intricate. In the following part we discuss how to evaluate the transmission fidelity for this protocol.

5.1 Fidelity of transmission for two-qubit encoding state transfer

Before discussing the figure of merit for the transmission quality let us comment on the operations needed for effectively realising the two-qubit encoding. If the initial state of qubit 2 is $|0\rangle$ (respectively $|1\rangle$) then the encoding of the initial state into ρ_{12}^- (respectively ρ_{12}^+) is obtained simply using the CNOT gate: $\text{CNOT} = \frac{1+\sigma^z}{2} \otimes 1 + \frac{1-\sigma^z}{2} \otimes \sigma^x$. In order to better illustrate the decoding procedure, without loss of generality we assume that the initial state of qubit 2 is the completely mixed state; different initial states can be tackled in a similar way. Let \mathcal{C}^\pm be the quantum operation realising the encoding, i.e.

$$\rho_{12}^\pm = \mathcal{C}^\pm \left[\rho_1(0) \otimes \frac{1_2}{2} \right], \quad \Longrightarrow \quad \sigma_{\pm,12}^\alpha = \mathcal{C}^\pm [\sigma_1^\alpha \otimes 1_2] / 2. \quad (35)$$

Such a quantum operation cannot be a unitary gate, as the eigenvalues of the input and output operators are different (two eigenvalues of ρ_{12}^\pm are null). Let us consider for instance the preparation of ρ_{12}^+ : One can measure σ_2^z , flip the state of qubit 2 depending on the result, and then apply the unitary CNOT gate. Another possibility, which does not involve measurements, is to apply a local completely positive map \mathcal{P} such that $\mathcal{P}[\rho_1 \otimes \rho_2] = \rho_1 \otimes |1\rangle\langle 1|$ and then apply a CNOT gate. In this particular case the encoding reads

$$\mathcal{C}^+[\rho] = \sum_{i=1}^2 \text{CNOT} (1 \otimes A_i) \rho (1 \otimes A_i^\dagger) \text{CNOT} \quad (36)$$

where we have chosen a particular set of Kraus operators realising the map \mathcal{P} : $A_1 = \frac{1+\sigma^z}{2}$, and $A_2 = \sigma^-$.

We now investigate the necessary decoding quantum operation. As shown in Section 2, in order to evaluate the transmission fidelity one has to obtain the matrix elements $D_{\alpha\beta}(t)$ which define the linear relation between the initial Bloch vector, with elements $r_1^\beta(0)$, and the final evolved Bloch vector, whose elements $r_N^\alpha(t) = \langle \sigma_N^\alpha(t) \rangle$ describe the state of the last qubit at time t . After having applied the encoding (36) we suppose that the elements $D_{\alpha\beta}(t)$ can be made independent of the parity, and in general independent of $|\Psi_{\bar{r}}(0)\rangle$, via a suitable decoding quantum operation \mathcal{D}^\pm . Let us write $r_N^\alpha(t)$ explicitly:

$$r_N^\alpha(t) = \text{Tr}[\sigma_N^\alpha \rho(t)] = \text{Tr} \left(\sigma_N^\alpha \mathcal{D}_{N,N-1}^\pm [e^{-iHt} \mathcal{C}_{12}^\pm [\rho(0)] e^{iHt}] \right) \equiv \text{Tr} \left(e^{iHt} \tilde{\mathcal{D}}_{N,N-1}^\pm [\sigma_N^\alpha \otimes 1] e^{-iHt} \mathcal{C}_{12}^\pm [\rho(0)] \right), \quad (37)$$

where $\tilde{\mathcal{D}}$ is the dual quantum operation, i.e. if $\mathcal{D}[\rho] = \sum_i D_i \rho D_i^\dagger$ then $\tilde{\mathcal{D}}[\rho] = \sum_i D_i^\dagger \rho D_i$. The subscripts in the above equation are used when we want to make explicit on which qubit the codes act; moreover we frequently switch from the

Heisenberg to the Schrödinger picture. In principle it would be tempting to set $\tilde{\mathcal{D}}^\pm = \mathcal{C}^\pm$. Indeed, if this were possible then $\tilde{\mathcal{D}}_{N,N-1}^\pm[\sigma_N^\alpha \otimes 1] = \sigma_{\pm,N,N-1}^\alpha$, namely one could write $r_N^\alpha(t) = \langle \sigma_{\pm,N,N-1}^\alpha(t) \rangle$ and make the map independent of the parity of the chain. However, this is not feasible in general: For instance if one sets $\tilde{\mathcal{D}}^+ = \mathcal{C}^+$ with the encoding (36), then the physical operation \mathcal{D}^+ , which is the real operation performed onto the state, would not be a physical trace-preserving completely positive map. One could implement the decoding by measuring the qubit $N-1$, in a way similar to what has been described for realising the encoding operation. However, in this case the mapping is not linear, as in Eq. (7), and it may be much more complicated to obtain the transmission fidelity.

We consider here a simple decoding procedure. We do not claim that this is the optimal procedure, and we argue that, for increasing the fidelity, one could find a better combination of local encoding/decoding protocols such that the encoded and decoded two-qubit states depend only on pairs of local fermionic operators and not on the parity. Here we assume that the initial state is encoded into the state ρ_{12}^+ . As for the decoding operation, we simply apply the CNOT gate to the qubits N and $N-1$. With a long but straightforward calculation one can evaluate the matrix $D(t)$ which describes the transmission channel (see Section 2)

$$D(t) = \begin{pmatrix} \Re[U_{N,1}(t)U_{N-1,2}(t) - U_{N-1,2}^2] & \Im[U_{N,1}(t)U_{N-1,2}(t) - U_{N-1,2}^2] & \Re[(U_{N,1}(t) + U_{N-1,2}(t))U_{N-1,2}^*] \\ -\Im[U_{N,1}(t)U_{N-1,2}(t) - U_{N-1,2}^2] & \Re[U_{N,1}(t)U_{N-1,2}(t) - U_{N-1,2}^2] & \Im[(-U_{N,1}(t) + U_{N-1,2}(t))U_{N-1,2}^*] \\ 0 & 0 & |U_{N,1}(t)|^2 + |U_{N-1,1}|^2 \end{pmatrix}, \quad (38)$$

where we have used the property $U_{1,N-1} = U_{2,N}$ which follows from mirror symmetry. Note that $\det D(t) > 0$ for every time t . On the other hand, mappings such that $\det D(t) < 0$ are not suitable for transferring quantum information, as the resulting fidelity is always lower than the classical value [52]. The final analytical expression for the optimal transmission fidelity F_e for the two qubit protocol is rather complicated. An approximated formula can be obtained assuming the optimal dynamics: as the aim of the optimal dynamics is to maximise $|U_{1,N}(t^*)|$ one can assume that $|U_{1,N-1}(t^*)| \approx 0$. Thanks to this approximation one obtains

$$F_e(t^*) \simeq \frac{1}{2} + u_1(t^*) \left(\frac{u_1(t^*) + 2u_2(t^*)}{6} \right), \quad u_1(t) = |U_{1,N}(t)|, \quad u_2(t) = |U_{2,N-1}(t)|. \quad (39)$$

The above expression shows that the maximization of $u_1(t^*)$ is, as expected, not enough for the two-qubit encoding protocol: since two states have to be transferred to the opposite side, the state of qubit 1 to qubit N and the state of qubit 2 to qubit $N-1$, one also has to find a proper scheme for maximizing $u_2(t^*)$ at the same time. In the following section we will use a minimally engineered chain for achieving this goal.

5.2 Minimal engineering for two-qubit state transfer

We have shown that, thanks to the two-qubit encoding, an XX spin chain can be used as reliable communication channel irrespective of the initial state of the chain, provided that it is able to transfer the state of qubits 1 and 2 to the state of qubits N and $N-1$ at the same transmission time t^* (see also [49] for a different, time dependent protocol). As the spin chain has to swap only the states of the four boundary qubits, irrespective of what happens to the bulk qubits, it turns out that the full engineering of the chain is, again, not required. We first use a minimal scheme, namely we use a setup which does not require further experimental control in addition to that needed for the encoding and decoding procedures. We show that the fidelity of transmission exceeds 89% in the infinite chain limit. Moreover, by introducing a further parameter we can achieve a transmission fidelity higher than 99% for chains where $N \lesssim 500$.

The encoding/decoding procedure illustrated in Section 5.1 avoids the destructive interference between the state to be transferred and the excitations inside the bulk. The price to be paid is the full control of the first two and last two qubits of the chain, as illustrated in Fig. 4. We argue accordingly that no more complications are introduced in requiring that the couplings $j_1 = j_{N-1}$ and $j_2 = j_{N-2}$ can be switched on and set to a particularly tuned value, while the rest of the qubits are permanently coupled with a homogeneous interaction strength j ($j = 1$ for convenience). This model with two parameters has already been introduced in [24] with a different aim, i.e. for improving the transmission capability of an XX spin chain, without any encodings. Indeed, we have shown in Section 3 that, with a single parameter, the two competing effects for obtaining coherent ballistic dynamics cannot be optimized simultaneously and one has to choose a compromise. On the other hand, in [24] it has been shown that using two parameters these two constraints can be satisfied independently. Due to the lack of the encoding/decoding algorithm, that scheme is suitable only for particular initial states of \tilde{I} , and optimizes just the transmission from site 1 to site N , i.e. from the sender to the receiver. The figure of merit for the transmission quality is given by Eq. (9), with $v_1(t) \equiv 0$ while $u_1(t)$ is given by (17). Although the analytic expressions for $\varrho(q)$ and ω_q are slightly complicated because of j_1 and the further parameter j_2 , one can analytically prove that $F > 99\%$ for $N \rightarrow \infty$. The resulting fidelity of state transmission is therefore almost perfect for every N .

Table 1. Transmission fidelity (9) at the transmission time t^* , for different length N , and with the optimal couplings. The left table refers to the cases discussed in [24], where j_1 and j_2 are set to their optimal values. In the right table on the other hand one also optimizes j_3 allowing a higher value of $u_2(t^*)$ and accordingly a higher fidelity.

N	t^*	j_1	j_2	$F_e(t^*)$	t^*	j_1	j_2	j_3	$F_e(t^*)$	$u_1(t^*)$	$u_2(t^*)$
20	26.5	0.550	0.818	0.987	27.8	0.503	0.709	0.880	0.998	0.999	0.994
30	37.7	0.497	0.781	0.979	39.4	0.448	0.648	0.846	0.996	0.999	0.991
50	59.5	0.434	0.735	0.970	61.8	0.386	0.575	0.803	0.995	0.998	0.987
70	80.9	0.397	0.706	0.964	83.6	0.349	0.529	0.775	0.994	0.998	0.985
100	112.5	0.359	0.675	0.958	115.8	0.313	0.483	0.744	0.993	0.998	0.983
150	164.7	0.320	0.641	0.951	168.6	0.276	0.434	0.710	0.993	0.998	0.982
250	267.8	0.276	0.599	0.944	272.7	0.236	0.378	0.667	0.992	0.998	0.980
350	370.2	0.250	0.572	0.939	375.9	0.212	0.344	0.640	0.992	0.998	0.979
500	523.0	0.225	0.544	0.935	529.6	0.189	0.310	0.611	0.991	0.998	0.978

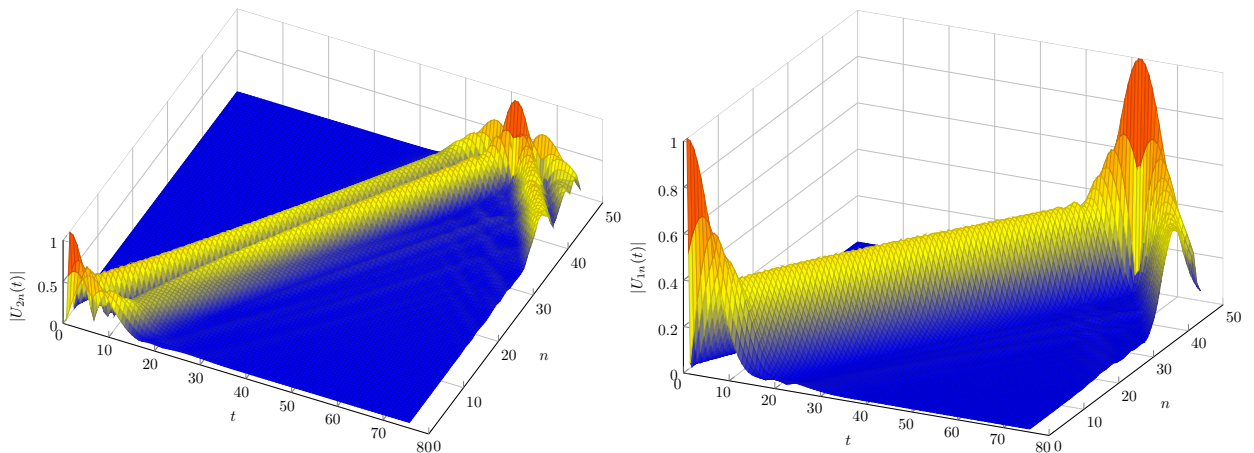


Fig. 5. Evolution operators $U_{1n}(t)$ and $U_{2n}(t)$ for different position n and time t . The wave-like motion displays the coherent excitation traveling from site 2 to site $N - 1$ (left) and from site 1 to site N (right). An almost perfect reconstruction of the states occurs at the opposite sides when the optimal couplings are used. Here $N = 50$ and the optimal couplings are shown in Table 1.

Here we use that scheme for studying quantum state transfer with the two-qubit encoding protocol. In this case, Eq.(39) shows that the efficient transmission of one fermion from site 1 to N is not enough and also the transmission from site 2 to site $N - 1$ has to be optimal. Although the minimal engineering scheme with the two parameters j_1 and j_2 derived in [24] has not been designed for this purpose, Table 1 shows that the final transmission quality $F_e(t^*)$ is very good. Thanks to the analytical results available [43,24] one can estimate the value of $F_e(t^*)$ for $N \rightarrow \infty$. Indeed

$$u_1(t^*) \approx \left| \sum_q \varrho(q) e^{i[Nq - \omega_q t^*]} \right| \stackrel{N \rightarrow \infty}{\simeq} 0.987, \quad u_2(t^*) \approx \left| \sum_q \frac{\omega_q^2}{j_1^2} \varrho(q) e^{i[Nq - \omega_q t^*]} \right| \stackrel{N \rightarrow \infty}{\simeq} 0.712, \quad (40)$$

from which one estimates $F_e(t^*) \approx 89.7\%$ for $N \rightarrow \infty$. The first result in the above formula has been obtained in [24] while the second one has been obtained by using the identities known for tridiagonal matrices [43] and going to the continuum limit. The lower value of $u_2(t^*)$ can be improved by numerically optimizing j_1 and j_2 in order to maximize both $u_1(t^*)$ and $u_2(t^*)$. However, the results obtained are not significantly better: even if one tries to maximise $u_2(t^*)$ alone, one obtains $u_2(t^*) \approx 0.732$ in the thermodynamic limit.

Almost perfect transmission for very long chains can be obtained by adding a further parameter j_3 to be optimized. As shown in Table. 1, thanks to this further parameter one can obtain a fidelity higher than 99% for chains as long as 500 qubits. The introduction of this further parameter guides the creation of a coherent wave-packet both from site 1 and from site 2. As shown in Fig. 5 the excitation travelling from site 2 generates two wave-packets. The first wave-packet goes towards site 1, where it is reflected from the boundary, and then goes towards to the opposite end. The second wave-packet on the other hand goes directly towards the opposite boundary, where it is reflected. Thanks to the optimized constructive interference, these two wave-packets come together in site $N - 1$ at the transmission time with a probability $u_2(t^*) \approx 98\%$ for chains up to $N = 500$. When this three-parameter optimization is used the transmission times are slightly longer, though they are still comparable with the previously obtained ballistic times (see Table 1).

Without the two-qubit encoding there is a temperature threshold, depending on the gap of the Hamiltonian, above which the transmission quality is suppressed [46], though no significant alterations are expected in the dynamics of the z component of the magnetization [50]. In this section we have shown that with a two-qubit encoding one can reliably transfer quantum information with minimal engineered chains even in the infinite temperature regime.

6 Towards experimental realizations

The ballistic approach to state transfer using minimally engineered models has been guided all along by the quest for experimental simplicity; however, there are some theoretical simplifications that must be overcome in looking for possible implementations. Some general imperfections in the transfer scheme may arise irrespective of the specific setup, such as the gradual (non-sudden) switching of the coupling between the sender (receiver) qubit and the bus, or the role of spurious interactions. In [38] it has been shown that a linear switching of j_1 from 0 to j_1^{opt} does not alter significantly the transmission quality, provided that the switching time is smaller than $1/j_1^{\text{opt}}$. Another experimentally relevant feature is that the overall “reading time” t_R , i.e. the interval during which the state remains at the receiver site, is finite, as seen for instance in Fig. 5. In the optimal regime [22], the transfer time scales with the system size as $t^* \approx N + 2.3N^{1/3}$ while the “reading time” increases with N according to the asymptotic behaviour $t_R \approx 1.9N^{1/3}$. As a result, the quantum channels based on the optimal transfer scheme might be embedded also in a macroscopic setups.

Another detrimental effect can arise from the interaction between quasi-particles due to residual non-quadratic terms in the Hamiltonian that cannot be completely screened out. These effects are investigated [38] with an XXZ model. It is found that the introduction of a coupling J^z along the z direction between adjacent spins evidently affects the quality of the channel. In fact, it weakly deteriorates the fidelity when $|J^z| < 0.2$, while the negative effects of this interaction are more pronounced for $J^z < -0.2$. Moreover, the effect of static noise in the coupling strength has been investigated in [53,54]. A non-uniform deviation is introduced in the couplings of the internal chain, $j_n \simeq 1 + \delta_n$, $\delta_n \ll 1$, while the optimal parameters are supposed not to be affected by imperfections. It is shown that the quality of the transmission generated by the optimal couplings weakly deteriorates when $|\delta_n| \lesssim 0.05$. When the strength of the imperfections is stronger the performance of minimally engineered chains is comparable to that of fully engineered ones. If disorder cannot be avoided, the full engineering of the chain is therefore unnecessary, as minimally engineered models, which are easier to implement in an experiment, have comparable transmission fidelities. On the other hand, imperfect tuning of the optimal parameters does not significantly alter the transmission quality. For instance, in Fig. 2 (see also [22]) one can see that there is an optimal region around the optimal values where the fidelity remains very high.

In addition to the imperfections described above, whose effects depend on the particular setup, there can also be other specific ones. As a matter of fact, in order to use many-body dynamics for transferring quantum information, long coherence times are required, together with the ability of performing single-site addressing and time-dependent measurements. An imperfect implementation of these requisites could introduce further error sources. Understanding whether a currently established experimental apparatus can be used as a coherent ballistic quantum data-bus is complicated, as one has to fathom if the various requisites might be somehow achieved in the near future.

In [18,55] a chain of coupled nitrogen-vacancy (NV) defects in diamonds has been proposed to operate as a high-quality transmission wire, provided that $j_1 \ll 1$. In [56] a thorough analysis of the role of the typical decoherence times found in experiments has shown that a NV-wire can act as an entanglement transmission channel. It is there showed that non-perturbative couplings to the wire are favorable, so one is inclined to think that the techniques developed in this paper may help the design of proper experimental setups based on NV centers.

Cold atom experiments [57,58,59,60,61,62,63] are now established *quantum simulators*; they can effectively implement a spin chain and seem the most convenient for testing the predictions of this paper. They have long coherence times, operating practically at zero temperature and without decoherence. For this reason, in [38] we have put forward a promising possible experimental realization using cold atoms trapped in optical lattices and near field Fresnel trapping potentials.

Nuclear magnetic resonance experiments are also promising candidates for simulating quantum information transport [50,64,65,66,67,68]. However, their highly mixed (high-temperature) initial state prevents the possibility of using such a setup for transferring superpositions of quantum states without any other control on the system. Coherent transmission of quantum superpositions can, in principle, be performed using the two-qubit encoding and engineering proposed in Section 5.2 provided that local gates acting on the boundaries can be implemented in the experimental setting. Despite the difficulties in maintaining the phase coherence required for transferring quantum superposition of states, some results of the present paper might be observed even with currently available technology. Indeed, the wave-packet generated by the two “classical” states $|0\rangle$ and $|1\rangle$ survives, and it is not altered, even at finite temperature. The corresponding wave-like evolution [24] can then be observed by measuring the magnetization along the z direction $\langle \sigma_n^z(t) \rangle$. The coherent magnetization dynamics allows the transmission of the two *classical* states $|0\rangle$ and $|1\rangle$, irrespective of what happens to their superposition, making the spin-wire still useful for classical information transfer.

7 Concluding remarks

High-quality quantum state transmission between distant qubits can be obtained via the dynamics of a spin chain according to several different schemes. The one here reviewed relies on the optimization of the interactions between the boundaries (where the sender's and receiver's qubits are located) and the spin-chain bus. Once such couplings are properly chosen, the excitations with linear dispersion relation get to rule the dynamics and a coherent ballistic transmission is consequently obtained. The procedure does not require any further design either of the bus, or of its initial state. When the approach is implemented with the spin-1/2 XX and XY models, the problem can be mapped to the optimization of a Fermionic quantum walk in one dimension.

Due to the induced ballistic dynamics, the transfer time scale is considerably shorter than in previous works [7, 16, 69, 70, 71]. It essentially depends on the group velocity of the elementary excitations, which can be tuned by varying the global parameters of the data-bus, namely the anisotropy γ and the magnetic field h . The optimal average fidelity, namely the figure of merit used for measuring the transmission quality, in the optimal regime only slightly deteriorates as the length of the bus increases.

A two qubit encoding protocol based on the optimal dynamics can also be designed such that the destructive effects of a (possible) thermal bath are overcome. The transfer quality is investigated using a specific figure of merit which takes into account the two-qubit encoding protocol. It turns out that the maximization of the transfer quality requires the optimization of the dynamics so that the states of qubit 1 and 2 are transmitted to the states of qubits N and $N - 1$. A minimal engineering which does not require further control on the system is then introduced to achieve this goal. The proposed protocol permits to reliably perform quantum state transmission even at infinite temperature.

Acknowledgements

The author thanks B. Antonio, T.J.G. Apollaro, A. Bayat, S. Bose, A. Cuccoli, R. Vaia and P. Verrucchi for interesting discussions and insightful comments. The author is currently supported by the ERC grant PACOMANEDIA.

A Diagonalization of quadratic Fermi Hamiltonian

The Hamiltonian (1) can be written in the form

$$H = \frac{1}{2} \eta^\dagger S \eta + \frac{1}{2} \text{Tr} A, \quad S = \begin{pmatrix} A & B \\ -B & -A \end{pmatrix}, \quad (41)$$

where $\eta_i = c_i$, $\eta_{i+N} = c_i^\dagger$ and $i = 1, \dots, N$. In [10, 72] it is shown that the above Hamiltonian can be diagonalized via a canonical transformation and written in the form

$$H = \frac{1}{2} \eta^\dagger \begin{pmatrix} P & Q \\ Q & P \end{pmatrix}^T \begin{pmatrix} \omega & 0 \\ 0 & -\omega \end{pmatrix} \begin{pmatrix} P & Q \\ Q & P \end{pmatrix} \eta + \frac{1}{2} \text{Tr} A = \frac{1}{2} \eta'^\dagger \begin{pmatrix} \omega & 0 \\ 0 & -\omega \end{pmatrix} \eta' + \frac{1}{2} \text{Tr} A, \quad (42)$$

where the energies ω_k are diagonal and non-negative. That is, in terms of some diagonal Fermi operators $b_k = \eta'_k$, $b_k^\dagger = \eta'_{k+N}$, $k = 1, \dots, N$ the Hamiltonian takes the form $H = \sum_k \omega_k b_k^\dagger b_k + \frac{1}{2} \text{Tr}(A - \omega)$. This transformation diagonalizing the Hamiltonian can be obtained from a singular value decomposition [34] and written as

$$A - B = \Phi^T \omega \Psi, \quad P = (\Phi + \Psi)/2, \quad Q = (\Phi - \Psi)/2. \quad (43)$$

where Ψ, Φ are orthogonal matrices and ω diagonal and non-negative. The time evolution (4) follows from the calculation of the canonical transformation e^{-itS} and reads [10]

$$U(t) = P^T e^{-i\omega t} P + Q^T e^{i\omega t} Q, \quad V(t) = P^T e^{-i\omega t} Q + Q^T e^{i\omega t} P. \quad (44)$$

A.1 Mirroring conditions for XY models

A complication of the XY model is that the corresponding fermionic Hamiltonian does not conserve the number of particles. In this case the perfect mirroring condition reads $U(t^*) = e^{i\alpha} X$ and $V(t^*) = 0$, i.e.

$$\begin{pmatrix} P^T & Q^T \\ Q^T & P^T \end{pmatrix} \begin{pmatrix} e^{-iEt^*} & 0 \\ 0 & e^{iEt^*} \end{pmatrix} \begin{pmatrix} P & Q \\ Q & P \end{pmatrix} = \begin{pmatrix} e^{i\alpha} X & 0 \\ 0 & e^{-i\alpha} X \end{pmatrix} \equiv \hat{X}.$$

As in the XX case, this means that the matrix on the r.h.s. of the above equation can be diagonalized using the same matrices P and Q , and that the energy-eigenvalues have to satisfy the condition (15). Accordingly one must impose $[S, \hat{X}] = 0$, i.e. that $X A X = A$, $X B X = e^{2i\alpha} B$. The matrix A has to be persymmetric while there is still some freedom in the symmetry properties of B . As B is real the parameter α , which in the $B = 0$ case is a free parameter, has to be a multiple of $\frac{\pi}{2}$: the matrix B thus has to be persymmetric, when for instance $\alpha = \frac{\pi}{2}$ or anti-persymmetric, i.e. $\gamma_{N-n} = -\gamma_n$, when for instance $\alpha = \pi$. The physical origin of these constraints is still unclear, but there is an argument supporting the persymmetric case $\alpha = \frac{\pi}{2}$. Indeed, the XY model does not conserve the number of particles and the phase $(-1)^{\frac{\bar{n}(\bar{n}-1)}{2}}$ in (13) is not a constant of motion. However, the parity is conserved and $(-1)^{\frac{\bar{n}(\bar{n}-1)}{2}} e^{i\pi\bar{n}/2} = e^{i\pi\bar{n}^2/2}$ has a fixed value in each sector with constant parity. In the persymmetric case insofar, the dynamics effectively mirrors the state $|\psi\rangle$ without relative phases when the initial state has a definite parity.

We now generalize Lemma 2 of Ref. [12] for showing that, even in the less stringent case of perfect transmission only between the boundary qubits (irrespective of the bulk), the Hamiltonian has to satisfy some symmetries, and as a particular case it can be persymmetric. Indeed, let us assume that

$$\begin{pmatrix} P^T & Q^T \\ Q^T & P^T \end{pmatrix} \begin{pmatrix} e^{-iEt^*} & 0 \\ 0 & e^{iEt^*} \end{pmatrix} \begin{pmatrix} P & Q \\ Q & P \end{pmatrix} e_1 = e^{i\alpha} e_N ,$$

being e_i the vector with components $(e_i)_j = \delta_{ij}$. Then it must hold

$$e^{-i\omega_k t^*} P_{k1} = e^{i\alpha} P_{kN}, \quad e^{i\omega_k t^*} Q_{k1} = e^{i\alpha} Q_{kN}, \quad \forall k .$$

In particular, this reveals that $P_{k1}^2 = P_{kN}^2$, $Q_{k1}^2 = Q_{kN}^2$, and $P_{k1} Q_{k1} = e^{2i\alpha} P_{kN} Q_{kN}$. Again the above constraints are satisfied only if α is a multiple of $\pi/2$. By rising the Hamiltonian matrix S of (41) to an integer power, m , we can relate

$$e_1^T S^m e_1 = \sum_k \omega_k^m (P_{k1}^2 + (-1)^m Q_{k1}^2) = e_N^T S^m e_N, \quad e_{N+1}^T S^{2m} e_1 = 2 \sum_k \omega_k^{2m} (P_{k1} Q_{k1}) = e^{i2\alpha} e_{N+N}^T S^{2m} e_N . \quad (45)$$

For $m = 1$, this gives that $h_1 = h_N$. For $m = 2$, we find that $J_1^2 - J_{N-1}^2 + \gamma_1^2 - \gamma_{N-1}^2 = 0$ and $J_1 \gamma_1 + e^{2i\alpha} J_{N-1} \gamma_{N-1} = 0$, i.e. that $j_1 = j_{N-1}$ and $\gamma_1 = -e^{2i\alpha} \gamma_{N-1}$. Each time that m is increased by 1, new variables are introduced on each side of the equation. Since these sides must be equals the required symmetry properties follow. In particular we find that B has to be persymmetric for $\alpha = \pi/2, 3\pi/2$ and anti-persymmetric for $\alpha = 0, \pi$.

A.2 Reflection symmetry: mirror symmetric XY models

The reflection symmetry, or mirror-symmetry, occurs when the system is invariant under reflection, i.e. when the Hamiltonian does not change by exchanging the sites i and $N - i + 1$, being N the number of sites. Formally this means that $A_{i,j} = A_{N-j+1, N-i+1}$ and $B_{i,j} = B_{N-j+1, N-i+1}$, i.e.,

$$X A X = A^T = A, \quad X B X = B^T = -B, \quad (46)$$

being X the exchange matrix defined in (12). Matrices P satisfying the condition $X P X = P^T$ are also called persymmetric. One important property of persymmetric matrices is that $P X$ and $X P$ are symmetric, and thus can be diagonalized by standard eigenvalue decomposition. Let

$$(A - B) X = W^T \Omega W ,$$

be the eigenvalue decomposition of $(A - B)X$. Eq. (43) is obtained by setting $W = \Phi$, $\omega = |\Omega|$ and $\Psi = s W X$, where $s = \text{sign } \Omega$. Moreover, Eq. (A.1) for $\alpha = \pi/2$ impose that

$$\begin{pmatrix} P & Q \\ Q & P \end{pmatrix} \begin{pmatrix} X & 0 \\ 0 & -X \end{pmatrix} \begin{pmatrix} P & Q \\ Q & P \end{pmatrix}^\dagger = \begin{pmatrix} x^+ & 0 \\ 0 & x^- \end{pmatrix} ,$$

is diagonal, with diagonal x^+ and x^- . Explicit calculations show that if ω is ordered in increasing order, then $x^+ = -x^- = s$.

References

1. D. Press, T.D. Ladd, B. Zhang, Y. Yamamoto, *Nature* **456**(7219), 218 (2008)
2. C. Weitenberg, M. Endres, J. Sherson, M. Cheneau, P. Schauß, T. Fukuhara, I. Bloch, S. Kuhr, *Nature* **471**(7338), 319 (2011)
3. I. Chiorescu, Y. Nakamura, C.M. Harmans, J. Mooij, *Science* **299**(5614), 1869 (2003)
4. F. Schmidt-Kaler, H. Häffner, M. Riebe, S. Gulde, G.P. Lancaster, T. Deuschle, C. Becher, C.F. Roos, J. Eschner, R. Blatt, *Nature* **422**(6930), 408 (2003)
5. L.M. Vandersypen, M. Steffen, G. Breyta, C.S. Yannoni, M.H. Sherwood, I.L. Chuang, *Nature* **414**(6866), 883 (2001)
6. S. Bose, *Physical review letters* **91**(20), 207901 (2003)
7. S. Bose, *Contemp. Phys.* **48**, 13 (2007)
8. M. Takahashi, *Thermodynamics of one-dimensional solvable models* (Cambridge University Press, 2005)
9. A. Bayat, S. Bose, *Phys. Rev. A* **81**, 012304 (2010)
10. A. Bayat, L. Banchi, S. Bose, P. Verrucchi, *Physical Review A* **83**(6), 062328 (2011)
11. M. Christandl, N. Datta, A. Ekert, A. Landahl, *Physical review letters* **92**(18), 187902 (2004)
12. A. Kay, Arxiv preprint arXiv:0903.4274 (2009)
13. C. Di Franco, M. Paternostro, M. Kim, *Physical review letters* **101**(23), 230502 (2008)
14. R. Heule, C. Bruder, D. Burgarth, V.M. Stojanović, *Phys. Rev. A* **82**, 052333 (2010)
15. H. Haselgrove, *Physical Review A* **72**(6), 062326 (2005)
16. A. Wójcik, T. Luczak, P. Kurzyński, A. Grudka, T. Gdala, M. Bednarska, *Phys. Rev. A* **72**(3), 034303 (2005)
17. A. Wójcik, T. Luczak, P. Kurzyński, A. Grudka, T. Gdala, M. Bednarska, *Phys. Rev. A* **75**, 022330 (2007)
18. N.Y. Yao, L. Jiang, A.V. Gorshkov, Z.X. Gong, A. Zhai, L.M. Duan, M.D. Lukin (2010), 1011.2762
19. S. Lorenzo, T. Apollaro, A. Sindona, F. Plastina, *Physical Review A* **87**(4), 042313 (2013)
20. S. Paganelli, S. Lorenzo, T.J. Apollaro, F. Plastina, G.L. Giorgi, *Physical Review A* **87**(6), 062309 (2013)
21. L. Banchi, T.J.G. Apollaro, A. Cuccoli, R. Vaia, P. Verrucchi, *Phys. Rev. A* **82**(5), 052321 (2010)
22. L. Banchi, T. Apollaro, A. Cuccoli, R. Vaia, P. Verrucchi, *New Journal of Physics* **13**(12), 123006 (2011)
23. L. Banchi, T. Apollaro, A. Cuccoli, R. Vaia, P. Verrucchi, *Nanomaterials and Nanotechnology* **1**(1), 24 (2011)
24. T. Apollaro, L. Banchi, A. Cuccoli, R. Vaia, P. Verrucchi, *Physical Review A* **85**(5), 052319 (2012)
25. T.J. Apollaro, S. Lorenzo, F. Plastina, *International Journal of Modern Physics B* **27**(01n03) (2013)
26. M.A. Nielsen, I.L. Chuang, *Quantum Computation and Quantum Information* (Cambridge University Press, 2000)
27. A. Fujiwara, P. Algoet, *Phys. Rev. A* **59**, 3290 (1999)
28. R. Horodecki, M. Horodecki, *Phys. Rev. A* **54**, 1838 (1996)
29. G. Bowen, S. Bose, *Phys. Rev. Lett.* **87**, 267901 (2001)
30. M. Horodecki, P. Horodecki, R. Horodecki, *Phys. Rev. A* **60**, 1888 (1999)
31. D. Kretschmann, R.F. Werner, *New Journal of Physics* **6**(1), 26 (2004)
32. A. Koetsier, R.A. Duine, I. Bloch, H.T.C. Stoof, *Phys. Rev. A* **77**(2), 023623 (2008)
33. P. Barmettler, A.M. Rey, E. Demler, M.D. Lukin, I. Bloch, V. Gritsev, *Phys. Rev. A* **78**(1), 012330 (2008)
34. E. Lieb, T. Schultz, D. Mattis, *Ann. Phys.* **16**, 407 (1961)
35. M. Christandl, N. Datta, T.C. Dorlas, A. Ekert, A. Kay, A.J. Landahl, *Phys. Rev. A* **71**(3), 032312 (2005)
36. C. Albanese, M. Christandl, N. Datta, A. Ekert, *Physical review letters* **93**(23), 230502 (2004)
37. M. Yung, S. Bose, *Physical Review A* **71**(3), 032310 (2005)
38. L. Banchi, A. Bayat, P. Verrucchi, S. Bose, *Phys. Rev. Lett.* **106**, 140501 (2011)
39. A. Cantoni, P. Butler, *Linear Algebra Appl.* **13**, 275 (1976)
40. B.N. Parlett, *The Symmetric Eigenvalue Problem* (SIAM, Philadelphia, 1998)
41. M. Bruderer, K. Franke, S. Ragg, W. Belzig, D. Obreschkow, *Physical Review A* **85**(2), 022312 (2012)
42. C. Albanese, M. Christandl, N. Datta, A. Ekert, *Phys. Rev. Lett.* **93**(23), 230502 (2004)
43. L. Banchi, R. Vaia, *Journal of Mathematical Physics* **54**, 043501 (2013)
44. T.J. Osborne, N. Linden, *Phys. Rev. A* **69**(5), 052315 (2004)
45. H.L. Haselgrove, *Phys. Rev. A* **72**(6), 062326 (2005)
46. L. Campos Venuti, C. Degli Esposti Boschi, M. Roncaglia, *Phys. Rev. Lett.* **99**(6), 060401 (2007)
47. C. Di Franco, M. Paternostro, D. Tsomokos, S. Huelga, *Physical Review A* **77**(6), 062337 (2008)
48. M. Markiewicz, M. Wieśniak, *Phys. Rev. A* **79**, 054304 (2009)
49. N.Y. Yao, Z.X. Gong, C.R. Laumann, S.D. Bennett, L.M. Duan, M.D. Lukin, L. Jiang, A.V. Gorshkov, *Physical Review A* **87**(2), 022306 (2013)
50. P. Cappellaro, L. Viola, C. Ramanathan, *Physical Review A* **83**(3), 032304 (2011)
51. A. Ajoy, P. Cappellaro, *Physical Review A* **85**(4), 042305 (2012)
52. P. Badziąg, M. Horodecki, P. Horodecki, R. Horodecki, *Phys. Rev. A* **62**, 012311 (2000)
53. A. Zwick, G. Álvarez, J. Stolze, O. Osenda, Arxiv preprint arXiv:1111.2238 (2011)
54. A. Zwick, G.A. Álvarez, J. Stolze, O. Osenda, arXiv preprint arXiv:1306.1695 (2013)
55. N.Y. Yao, L. Jiang, A.V. Gorshkov, P.C. Maurer, G. Giedke, J.I. Cirac, M.D. Lukin, *Nature Communications* **3**, 800 (2012)
56. Y. Ping, B.W. Lovett, S.C. Benjamin, E.M. Gauger, *Physical review letters* **110**(10), 100503 (2013)
57. W. Bakr, J. Gillen, A. Peng, S. Fölling, M. Greiner, *Nature* **462**(7269), 74 (2009)
58. G.K. Brennen, C.M. Caves, P.S. Jessen, I.H. Deutsch, *Phys. Rev. Lett.* **82**, 1060 (1999)

59. O. Mandel, M. Greiner, A. Widera, T. Rom, T. Hänsch, I. Bloch, Arxiv preprint quant-ph/0308080 (2003)
60. M. Greiner, O. Mandel, T. Esslinger, T.W. Hänsch, I. Bloch, Nature **415**, 39 (2002)
61. J. Sherson, C. Weitenberg, M. Endres, M. Cheneau, I. Bloch, S. Kuhr, Nature (2010)
62. W. Bakr, A. Peng, M. Tai, R. Ma, J. Simon, J. Gillen, S. Foelling, L. Pollet, M. Greiner, Science **329**(5991), 547 (2010)
63. M. Karski, L. Förster, J. Choi, A. Steffen, N. Belmechri, W. Alt, D. Meschede, A. Widera, New Journal of Physics **12**, 065027 (2010)
64. P. Cappellaro, C. Ramanathan, D. Cory, Physical review letters **99**(25), 250506 (2007)
65. C. Ramanathan, P. Cappellaro, L. Viola, D. Cory, New Journal of Physics **13**, 103015 (2011)
66. C. Ramanathan, P. Cappellaro, L. Viola, D. Cory, Arxiv preprint arXiv:1102.3400 (2011)
67. A. Ajoy, R.K. Rao, A. Kumar, P. Rungta, Physical Review A **85**(3), 030303 (2012)
68. K.R.K. Rao, A. Kumar, International Journal of Quantum Information **10**(04) (2012)
69. F. Plastina, T.J.G. Apollaro, Phys. Rev. Lett. **99**(17), 177210 (2007)
70. G. Gualdi, V. Kostak, I. Marzoli, P. Tombesi, Phys. Rev. A **78**(2), 022325 (2008)
71. S.I. Doronin, A.I. Zenchuk, Phys. Rev. A **81**(2), 022321 (2010)
72. J. Blaizot, G. Ripka, *Quantum theory of finite systems* (MIT Press, 1986), ISBN 9780262022149